Radiography 28 (2022) 95–101

Contents lists available at ScienceDirect

Radiography

journal homepage: www.elsevier.com/locate/radi

Amide proton transfer-weighted MRI in the clinical setting – correlation with dynamic susceptibility contrast perfusion in the post-treatment imaging of adult glioma patients at 3T

A.I. Friismose [a, *], L. Markovic [a], N. Nguyen [a], O. Gerke [b, c], M.K. Schulz [d], B.R. Mussmann [a, c, e, f]

[a] Radiology Department, Odense University Hospital, Odense, Denmark
[b] Department of Nuclear Medicine, Odense University Hospital, Odense, Denmark
[c] Department of Clinical Research, University of Southern Denmark, Odense, Denmark
[d] Department of Neurosurgery, Odense University Hospital, Odense, Denmark
[e] OPEN, Odense Patient Data Exploratory Network, Odense University Hospital, Odense, Denmark
[f] Faculty of Health Sciences, Oslo Metropolitan University, Oslo, Norway

ARTICLE INFO

Article history:
Received 25 June 2021
Received in revised form
13 August 2021
Accepted 19 August 2021
Available online 8 September 2021

Keywords:
Magnetic resonance imaging
Amides
Glioma
Perfusion
Cerebral blood volume
Brain neoplasms

ABSTRACT

Introduction: We investigated the correlation between amide proton transfer-weighted magnetic resonance imaging (APTw MRI) and dynamic susceptibility contrast (DSC) perfusion in order to assess the potential of APTw MRI as an alternative to DSC in adult brain tumor (glioma) imaging.
Methods: After Ethical Committee approval, forty adult patients, treated for histopathologically confirmed glioma (World Health Organization (WHO) grade II-IV), were prospectively imaged at 3 Tesla (3 T) with DSC perfusion and a commercially available three-dimensional (3D) APTw sequence. Two consultant neuroradiologists independently performed region of interest (ROI) measurements on relative cerebral blood volume (rCBV) and APTw maps, co-registered with anatomical images. The correlation APTw MRI-DSC perfusion was assessed using Spearman's rank-order test. Inter-observer agreement was evaluated by the intraclass correlation coefficient (ICC) and Bland-Altman (BA) plots.
Results: A statistically significant moderately strong positive correlation was observed between maximum rCBV ($rCBV_{max}$) and maximum APTw ($APTw_{max}$) values (observer 1: $r = 0.73$; $p < 0.01$; observer 2: $r = 0.62$; $p < 0.01$). We found good inter-observer agreement for $APTw_{max}$ (ICC = 0.82; 95% confidence interval (CI) 0.66–0.90), with somewhat broad outer 95% CI for the BA Limits of Agreement (LoA) (−1.6 to 1.9). ICC for $APTw_{max}$ was higher than ICC for $rCBV_{max}$ (ICC = 0.74; 95%; CI 0.50–0.86), but the difference was not statistically significant.
Conclusion: $APTw_{max}$ values correlate positively with $rCBV_{max}$ in patients treated for brain glioma. APTw imaging is a reproducible technique, with some observer dependence. Results need to be confirmed by a larger population analysis.
Implications for practice: APTw MRI can be a useful addition to glioma follow-up imaging and a potential alternative to DSC perfusion, especially in patients where contrast agent is contraindicated.

Introduction

Dynamic susceptibility contrast (DSC) perfusion is an advanced magnetic resonance imaging (MRI) technique, widely used in gliomas requiring surveillance.[1,2] DSC overcomes the lack of specificity of conventional contrast-enhanced MRI to discern between phenomena such as true progression, pseudoprogression and radionecrosis, which all affect blood brain barrier integrity, leading to contrast enhancement.[1,2] Relative cerebral blood volume (rCBV), obtained from DSC measurements, serves as a biomarker for tumor angiogenesis.[3] Although useful, DSC relies on gadolinium contrast, which increases the risk of nephrogenic systemic fibrosis in patients with impaired renal function and can accumulate in the brain

* Corresponding author. Odense University Hospital, Radiology Department, Kløvervænget 47, 5000, Odense, Denmark.
E-mail address: Ancuta.Ioana.Friismose@rsyd.dk (A.I. Friismose).

https://doi.org/10.1016/j.radi.2021.08.006

of patients with normal renal function after repeated administrations.[4] Moreover, DSC is prone to susceptibility artifacts at air-tissue interfaces, in the presence of surgical material and blood breakdown products.[3]

A variety of studies have been conducted investigating non-contrast, less susceptibility artifact prone alternatives to DSC.[5–7] Three-dimensional (3D) pseudo-continuous arterial spin labeling (pCASL) perfusion, susceptibility-weighted imaging (SWI) and dynamic contrast enhanced (DCE) (T_1) perfusion have shown significant correlations with DSC, fewer susceptibility artifacts and similar diagnostic performance in tumor grading and differentiating progression from treatment effects.[6,7]

Amide proton transfer-weighted MRI (APTw MRI) is a molecular imaging technique based on chemical exchange saturation transfer (CEST).[8] APTw signal reflects the concentration of protons in the amide groups (—NH) of mobile proteins and peptides and current evidence suggests APTw is positively correlated with cell density and proliferation.[9–11] APTw MRI has been applied in neuro-oncology (tumor grading, differentiating tumor recurrence from treatment effects), as well as in breast, prostate and cervical cancer.[12–16]

APTw MRI does not rely on exogenous contrast agent and may be a completely non-invasive alternative to DSC, especially in patients where contrast agent is contraindicated. APTw has also the practical advantage that acquisition can be immediately repeated if image quality is suboptimal, which is not the case with DSC perfusion.

Despite the promising results from studies investigating the use of APTw in conjunction with other advanced neuroimaging MR techniques such as DSC perfusion, intravoxel incoherent motion (IVIM) diffusion or spectroscopy, APTw MRI has not yet gained widespread clinical use.[12,17,18] With the APTw sequence now available as a commercial product, there is a need for further evidence regarding its implementation before incorporating APTw MRI into clinical imaging protocols.

APTw MRI has previously shown good repeatability in supratentorial locations, but inter-observer agreement was not investigated.[19]

The aim of the present study was therefore to assess the correlation between APTw MRI and DSC perfusion and the potential of APTw MRI as a non-contrast alternative to DSC perfusion in the imaging of adult glioma patients. Moreover, we performed inter-observer agreement analysis on APTw measurements.

Materials and methods

The investigators notified the Regional Research Ethics Committee and ethical approval was waived (Journal No. S-20182000-19), as the study was deemed non-interventional. Written informed consent was obtained from all participants and permission to handle patient data for research purposes was granted by the Danish Data Protection Agency (Journal No. 18/31,678).

Patients

Forty-one consecutive patients (mean 57 years, range 28–79, 14 female, 27 male), were imaged between October 2018–February 2019. One patient was excluded from analysis because of insufficient image quality.

The patients were referred for MRI as part of the follow-up routine or for treatment assessment. Inclusion in the study was based on the criteria: age over 18 and treated/under treatment for histopathologically confirmed glioma. Exclusion criteria were inability to provide informed consent, claustrophobia, pregnancy, MRI safety hazards and contrast agent contraindications. Patient enrolment details are provided in Fig. 1 and information about the included tumor types can be found in Table 1.

Image acquisition

Imaging was performed on a clinical 3 Tesla (3 T) MRI system (Achieva, Philips Medical Systems, the Netherlands), equipped with radio frequency (RF) MultiTransmit, using a 16-channel phased-array receive head coil.

A commercially available three-dimensional (3D) APTw sequence was added to the department's standard glioma follow-up protocol, consisting of anatomical sequences (3D fluid-attenuated inversion recovery (FLAIR), T_2, 3D T_1 pre- and post-contrast) and DSC perfusion.

DSC was performed as a T_2* weighted gradient-echo sequence with single-shot echo-planar imaging (EPI) readout (EPI factor 41) and fat suppression (spectral presaturation with inversion recovery (SPIR)), field of view (FOV) 224 × 224 mm^2, 25 contiguous slices, slice thickness 4 mm (100 mm axial coverage), in-plane resolution 2.3 × 2.3 mm^2 (reconstructed to 1.75 × 1.75 mm^2), repetition time (TR) 1606 ms, echo time (TE) 40 ms, flip angle 75°, 40 phases. Parallel imaging with a sensitivity encoding factor of 2.3 in the anterior posterior (AP) direction was used. Scan time was 1.09 min. A contrast bolus of 0.1 mL/kg Gadovist (gadobutrol, 1 mmol/mL, Bayer Healthcare, Germany) was administered with a flow of 2 mL/s via an i.v. catheter in the antecubital fossa, followed by a 35 mL saline flush.

APTw data was acquired pre-contrast from 10 contiguous axial slices, employing a 3D multishot turbo spin echo (TSE) sequence with lipid suppression (SPIR). Imaging parameters were: FOV 230 × 180 mm^2, in-plane resolution 1.8 × 1.8 mm^2 (reconstructed to 0.9 × 0.9 mm^2), slice thickness 6 mm (60 mm axial coverage), sensitivity encoding right left (RL) - 1.6, TR 6120 ms, TE 7.8 ms, flip angle 90°, TSE factor 174. APTw contrast parameters were RF saturation power 2 μT, saturation duration 2 s. Scan time was 3.46 min.

By using the two RF channels in an alternating fashion, a train of frequency-selective saturation RF pulses were applied at seven different frequency offsets, including the amide resonance frequency at +3.5 parts per million (ppm) relative to water (4.75 ppm). Three acquisitions with slightly different echo shifts (±0.5 ms) were performed at + 3.5 ppm in order to calculate an integrated B_0 map using the mDixon algorithm.[20]

The water signal level as a function of frequency offset was measured to generate a Z-spectrum, centered on the water resonance, assigned to 0 ppm. The saturated image (S_{sat}) and a non-saturated (S_0) image, acquired with a large RF pulse offset, were used to compute the magnetization transfer ratio asymmetry (MTR_{asym}) according to:[20]

$$MTR\_asym = (S\_sat(-3.5\ ppm) - S\_sat(3.5\ ppm)) / S\_0$$

APTw values span from −5% to +5% and represent the percentage signal change between the saturated and unsaturated image.

Image analysis

Images were analyzed independently by 2 consultant neuroradiologists with 10- and 25-years' experience, blinded to each other's measurements. The raters were not blinded to the histopathological grade of the tumors or the patients' clinical information. Each radiologist performed both rCBV and APTw measurements.

Perfusion maps (rCBV) were computed in IntelliSpace Portal v. 8 (Philips Healthcare, the Netherlands) using standard post-processing software. rCBV values were normalized to contralateral normal-appearing white matter (CNAWM) by choosing a

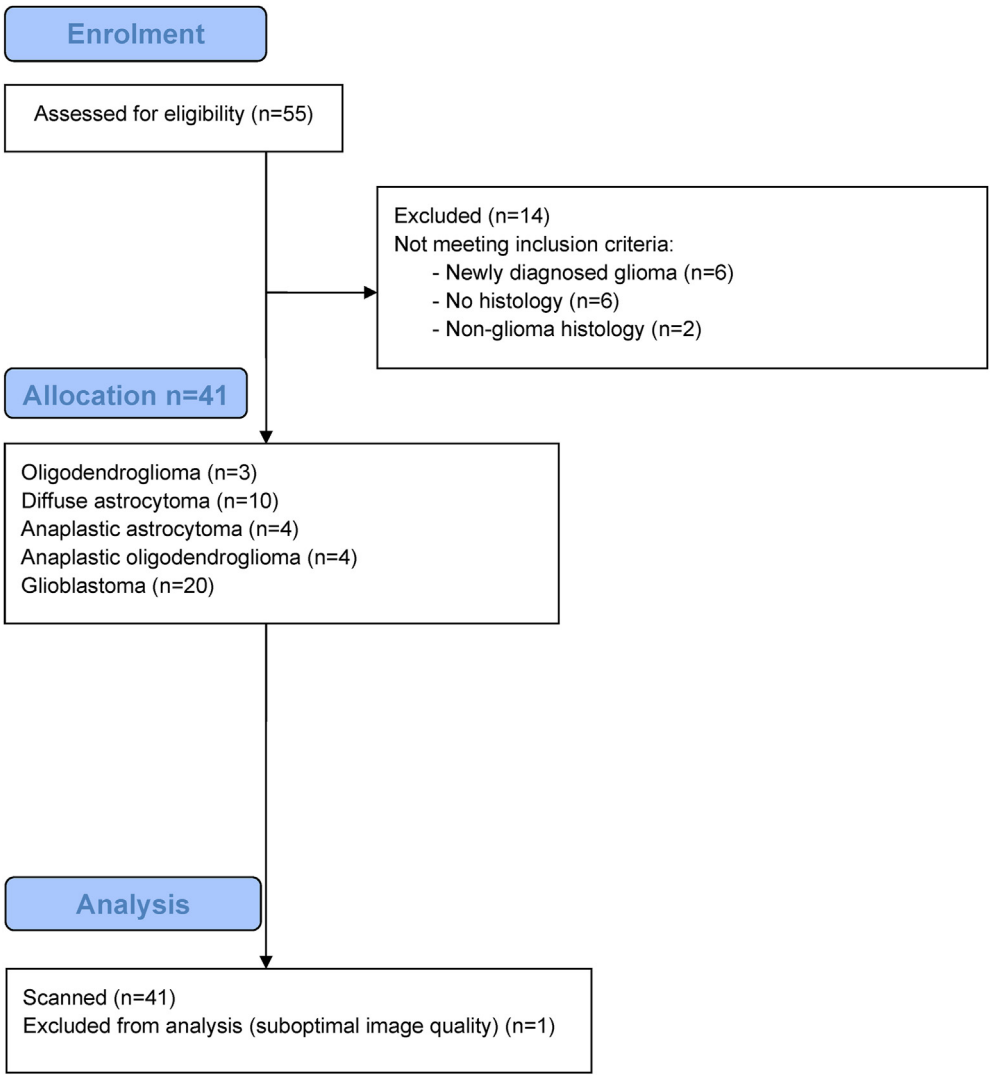

Figure 1. Flow chart describing the enrolment process, with details about excluded and included patients.

Table 1
Tumor histology, tumor grade and characteristics of the patients included in the study (n = 40).

Histology	Male (n)	Female (n)	Mean age years (range)
Oligodendroglioma (WHO II)	2	1	53 (44–60)
Diffuse astrocytoma (WHO II)	7	2	43 (28–60)
Anaplastic astrocytoma (WHO III)	3	1	53 (37–67)
Anaplastic oligodendroglioma (WHO III)	2	2	58 (46–71)
Glioblastoma (WHO IV)	12	8	64 (35–79)

WHO, World Health Organization.

region of interest (ROI) similar in size and located in the contralateral hemisphere. APTw maps were automatically generated on the scanner and exported to IntelliSpace.

Contrast-enhanced 3D T_1 and, for non-enhancing lesions, 3D FLAIR images were co-registered with the rCBV and APTw maps to provide anatomical information.

Each observer drew up to five ROIs per patient in areas which, upon visual inspection, either demonstrated contrast enhancement on post-contrast T_1 weighted images or had imaging features indicative of non-enhancing residual/recurring tumor on FLAIR. The APTw-rCBV ROI pairs for each patient had similar size and were placed in similar anatomical locations, based on visual assessment. Areas of necrosis, hemorrhage and large vessels were avoided. The ROI with the maximum value was chosen among the APTw and respectively the rCBV ROIs for each patient.

Statistical analysis

Maximum rCBV ($rCBV_{max}$) and maximum APTw ($APTw_{max}$) values were used in the statistical analysis. Spearman's rho (r) was computed for each observer and applied to test the strength of the relationship between $APTw_{max}$ and $rCBV_{max}$. Correlation coefficient values of 0.6–0.8 were considered moderately strong.[23]

The intraclass correlation coefficient (ICC) for the $APTw_{max}$ and $rCBV_{max}$ recorded by the two observers was computed based on a two-way random-effects model, mean rating (k = 2) and absolute agreement.[24] ICC values between 0.75 and 0.9 were considered to indicate good inter-observer agreement.[25] The inter-observer differences between $APTw_{max}$ and $rCBV_{max}$ were quantified by Bland-Altman (BA) plots, after testing for normality using the Shapiro–Wilk test. Visualizations were done with scatter plots, supplemented by supporting linear regression lines and 95% confidence bands.[26,27] Statistical significance was considered if

$p < 0.05$. Statistical analysis was performed using Stata IC/16 software (StataCorp LLC, College Station, TX).

Results

Correlation analysis

Spearman's rho showed a statistically significant moderately strong positive correlation between $APTw_{max}$ and $rCBV_{max}$. The correlation coefficients were $r = 0.73$; $p < 0.01$ for observer 1 and $r = 0.62$; $p < 0.01$ for observer 2. APTw signal intensity also seemed to correlate visually with rCBV as shown in Fig. 2 and Fig. 3.

The correlation between $APTw_{max}$ and $rCBV_{max}$ for each observer is illustrated in Fig. 4. No trend was observed between outliers on the scatter plots in Fig. 4 and a particular histology type.

Inter-observer agreement

ICC for $APTw_{max}$ was 0.82 (95% confidence interval (CI) 0.66–0.90), indicating good inter-observer agreement. ICC for $rCBV_{max}$ was 0.74 (95% CI 0.50–0.86). Due to the overlap between CI, the difference between the ICC for $APTw_{max}$ and the ICC for $rCBV_{max}$ couldn't be considered statistically significant.

The inter-observer Bland-Altman limits of agreement (LoA) were −1.27 to 1.49 and −2.84 to 2.73 for $APTw_{max}$ and $rCBV_{max}$, respectively. The outer 95% confidence limits for the LoA were −1.60 to 1.90 for $APTw_{max}$ and −3.70 to 3.60 for $rCBV_{max}$. The results of BA analysis are presented in Table 2 and Fig. 5.

Upon visual inspection of the BA plot, no trend was observed between the difference and the mean, with difference scores evenly distributed below and above the bias line within the 95% LoA.

Discussion

In our study, we investigated the correlation between APTw and rCBV values in post-treatment glioma, as well as inter-observer agreement for APTw measurements. We found a moderately strong positive correlation between $APTw_{max}$ and $rCBV_{max}$ values. The ICC showed good inter-observer agreement for APTw imaging, while the slightly broad outer 95% CI for the LoA on the BA plot indicated the APTw technique has some degree of observer dependence.

The potential of APTw in post-treatment glioma imaging has been investigated in pre-clinical and clinical studies.[28,29] The novelty of our study consists in the use of a commercially available APTw sequence and standard post-processing to assess the correlation between APTw and rCBV. Furthermore, we investigated inter-observer agreement for APTw measurements. This is – to our knowledge – a less documented aspect in the literature, but of considerable importance for the clinical implementation of APTw imaging.

The findings regarding the correlation between APTw and rCBV values agree with previous studies. Similar to our results, Togao et al. reported a positive correlation ($r = 0.42$, $p < 0.01$) between the 90th-percentile of APTw and rCBV values on histogram analysis in tumor grading.[17]

Our results indicated that APTw measurements are reproducible, but with some observer dependence, which could be explained by variations in ROI placement. In future studies, inter-observer agreement could potentially be improved by adopting a less user-dependent image analysis approach, such as histogram analysis, previously described in the literature.[30,31]

Based on BA analysis, $APTw_{max}$ showed less observer dependence than $rCBV_{max}$, which has been reported to vary not only with ROI placement, but also with variations in the choice of reference tissue used for normalization.[32,33]

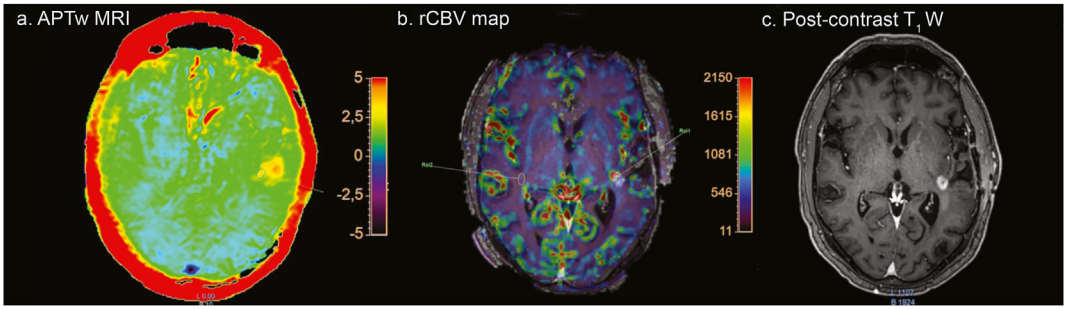

Figure 2. Patient with histopathologically confirmed glioblastoma, treated with surgery and chemoradiation. a. Amide proton transfer-weighted (APTw) image with hyperintense signal (APTw = 2.95%). b. Relative cerebral blood volume (rCBV) map with increased rCBV (3.34) relative to contralateral normal-appearing white matter (CNAWM). c. Enhancement on post-contrast T_1 weighted image.

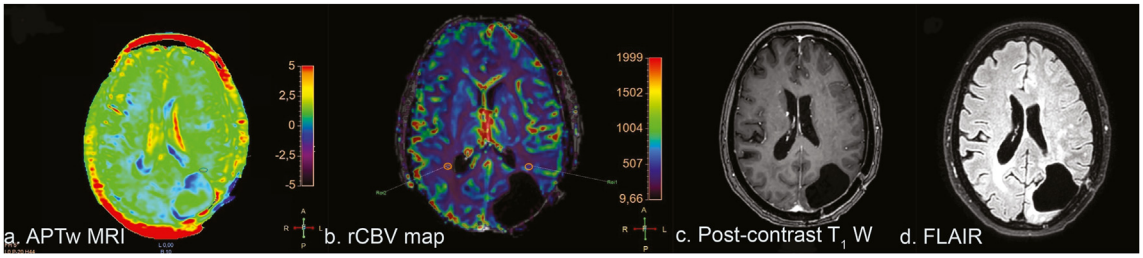

Figure 3. Patient with recurrent glioblastoma, treated with surgery, chemoradiation and anti-angiogenic therapy upon recurrence. a. Amide proton transfer-weighted (APTw) image with iso-to hypointense signal around the operation cavity (APTw = 0.15%). b. The relative cerebral blood volume (rCBV) map doesn't show significantly increased rCBV (1.41) relative to contralateral normal-appearing white matter (CNAWM). c. Post-contrast T_1 weighted image demonstrates no enhancement. d. FLAIR exhibits no sign of tumor progression.

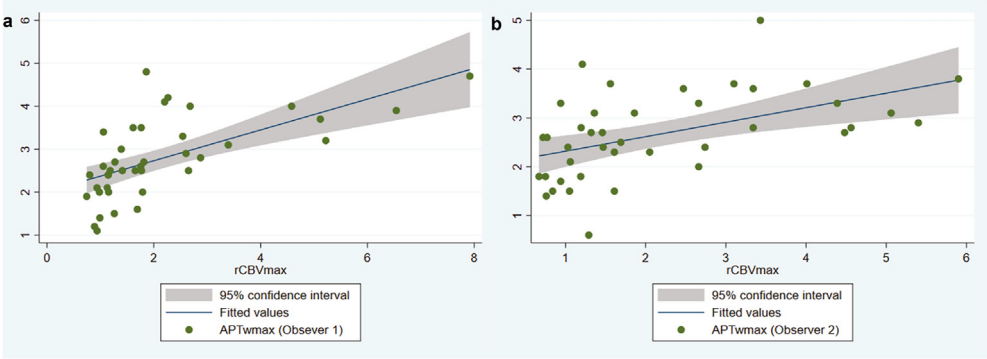

Figure 4. a. Correlation between maximum amide proton transfer-weighted ($APTw_{max}$) - maximum relative cerebral blood volume ($rCBV_{max}$) values for observer 1. b. Correlation $APTw_{max}$ - $rCBV_{max}$ for observer 2.

Table 2
Results of Bland-Altman analysis, showing inter-observer agreement for $APTw_{max}$ and $rCBV_{max}$.

	Bias Mean (SD)	Bias 95% CI	Limits of Agreement	Lower Limits of Agreement 95% CI	Upper Limits of Agreement 95% CI
$APTw_{max}$	0.11 (0.7)	−0.12 to 0.33	−1.27 to 1.49	−1.60 to −1.03	1.25 to 1.90
$rCBV_{max}$	−0.05	−0.51 to 0.40	−2.84 to 2.73	−3.70 to −2.36	2.25 to 3.60

$APTw_{max}$, maximum amide proton transfer-weighted value; $rCBV_{max}$, maximum relative cerebral blood volume; SD, standard deviation; CI, confidence interval.

Even though APTw and rCBV appear to be positively correlated, the techniques represent different contrast mechanisms, reflecting two hallmarks of tumor activity. The APTw effect is considered to originate from hypercellularity and increased concentration of amide protons in the cytoplasm of proliferating glioma cells, whereas rCBV is a marker of neovascularization.[13,34] It is therefore likely that APTw imaging provides additional information to rCBV and could potentially increase diagnostic accuracy in challenging situations. Evidence currently suggests that using APTw imaging together with DSC perfusion improves diagnostic performance when distinguishing between recurrent glioma and treatment-related effects.[28,30]

An interesting finding of our study was that the area of APTw signal hyperintensity measured in our cohort was generally larger than the corresponding rCBV and contrast-enhancing hotspots (Fig. 2). This phenomenon has previously been reported and attributed to the presence of tumor infiltration.[35] The ability of APTw MRI to detect tumor invasion beyond areas of increased rCBV and contrast enhancement might improve the sensitivity of post-treatment imaging to detect early tumor progression. This can be particularly challenging after anti-angiogenic therapy, where infiltrative non-enhancing progression has been observed.[36]

APTw vs. DSC parameters

The APTw and DSC sequences employed in this study used different in-plane spatial resolution, slice thickness and coverage.

DSC had lower in-plane spatial resolution compared to APTw (2.3×2.3 mm^2 vs. 1.8×1.8 mm^2), reflecting the need for acquisition speed to capture the first passage of contrast bolus through the vasculature.[21]

Because of the long RF saturation duration needed to achieve optimal image contrast and the acquisition of several frequency offsets to generate a Z spectrum, APTw used a long TR, resulting in

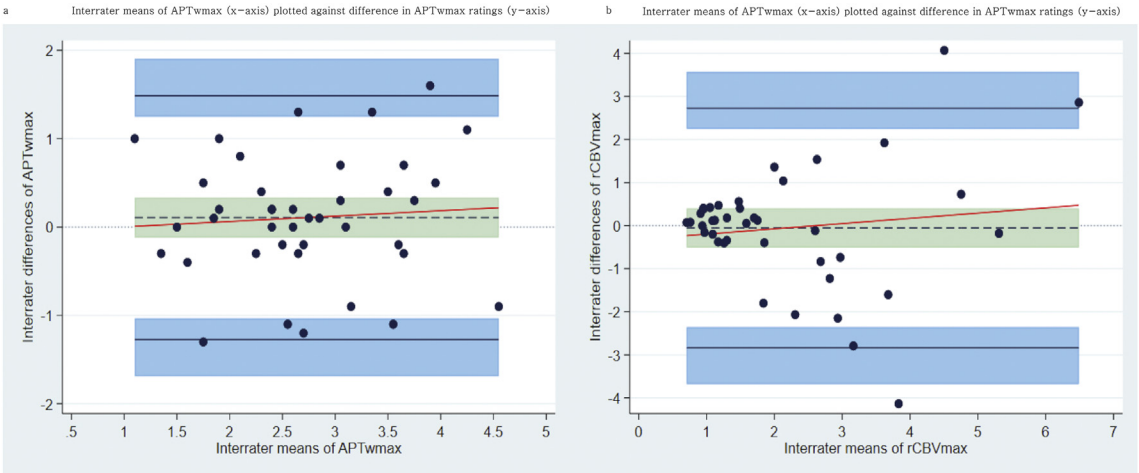

Figure 5. Bland–Altman plots visualizing inter-observer agreement for maximum amide proton transfer-weighted ($APTw_{max}$) and maximum relative cerebral blood volume ($rCBV_{max}$) values. Limits of Agreement (LoA) are represented as continuous black lines. Ninety-five confidence intervals (CI) for the bias and the LoA are indicated by olive and blue shaded areas, respectively. The regression line representing the fit between the differences and the mean is shown in red.

long scan times. To avoid prolonging scan time and minimize the risk of motion artifacts, lower coverage was employed for APTw (60 mm) compared to DSC (100 mm).

Moreover, APTw acquisition parameters had been experimentally optimized to maximize image contrast and modifying parameters carried the risk of influencing APTw values and sequence performance.[20,22]

Using identical in-plane spatial resolution, slice thickness and coverage for APTw and DSC could potentially improve comparability and have a positive effect on study results. However, this might come at the expense of increased scan time and potentially suboptimal image contrast, which would counteract the positive effects of increased comparability.

Limitations

While the present study contributes additional data to validate the correlation between APTw values and rCBV, it is based on a relatively small number of participants.

Furthermore, no intra-observer agreement analysis was performed and consequently, an estimation of APTw repeatability could not be made. Further investigation of intra-observer agreement to assess the robustness of the APTw sequence and comparison with existing repeatability studies is required. Further training in interpreting APTw maps and avoiding pitfalls could also improve agreement.

Assessing the clinical significance of APT's observer dependence was challenging, mostly because of the limited clinical experience with the technique and the lack of standardization of APTw imaging parameters. As APTw parameters (especially RF saturation scheme) can have an influence on APTw signal intensity, comparison with APTw values reported in the literature was difficult.[37]

The use of commercially available sequences will hopefully lead to a higher degree of standardization, facilitate comparisons among studies and encourage the adoption of APTw imaging as a clinical tool.

Conclusion

In conclusion, there is a statistically significant positive correlation between $APTw_{max}$ and $rCBV_{max}$ values in post-treatment gliomas, which makes APTw MRI a potentially valuable part of a multiparametric glioma imaging protocol. Moreover, the present study indicates that APTw imaging has good reproducibility, with some observer dependence. Results need to be confirmed by a larger population analysis.

Funding

This research did not receive any specific grant from funding agencies in the public, commercial, or not-for-profit sectors.

Conflict of interest statement

None.

Appendix A. Supplementary data

Supplementary data to this article can be found online at https://doi.org/10.1016/j.radi.2021.08.006.

References

1. Wen PY, Macdonald DR, Reardon DA, Cloughesy TF, Sorensen AG, Galanis E, et al. Updated response assessment criteria for high-grade gliomas: response assessment in neuro-oncology working group. *J Clin Oncol* 2010;**28**(11):1963–72. https://doi.org/10.1200/jco.2009.26.3541.
2. Ahmed R, Oborski MJ, Hwang M, Lieberman FS, Mountz JM. Malignant gliomas: current perspectives in diagnosis, treatment, and early response assessment using advanced quantitative imaging methods. *Canc Manag Res* 2014;**6**:149–70. https://doi.org/10.2147/CMAR.S54726.
3. van Dijken BRJ, van Laar PJ, Smits M, Dankbaar JW, Enting RH, van der Hoorn A. Perfusion MRI in treatment evaluation of glioblastomas: clinical relevance of current and future techniques. *J Magn Reson Imag* 2019;**49**(1):11–22. https://doi.org/10.1002/jmri.26306.
4. Gulani V, Calamante F, Shellock FG, Kanal E, Reeder SB. Gadolinium deposition in the brain: summary of evidence and recommendations. *Lancet Neurol* 2017;**16**(7):564–70. https://doi.org/10.1016/s1474-4422(17)30158-8.
5. Xu Q, Liu Q, Ge H, Ge X, Wu J, Qu J, et al. Tumor recurrence versus treatment effects in glioma: a comparative study of three dimensional pseudo-continuous arterial spin labeling and dynamic susceptibility contrast imaging. *Medicine* 2018;**96**(50). e9332-e.
6. Park MJ, Kim HS, Jahng GH, Ryu CW, Park SM, Kim SY. Semiquantitative assessment of intratumoral susceptibility signals using non-contrast-enhanced high-field high-resolution susceptibility-weighted imaging in patients with gliomas: comparison with MR perfusion imaging. *AJNR Am J Neuroradiol* 2009;**30**(7):1402–8. https://doi.org/10.3174/ajnr.A1593.
7. Saini J, Gupta RK, Kumar M, Singh A, Saha I, Santosh V, et al. Comparative evaluation of cerebral gliomas using rCBV measurements during sequential acquisition of T1-perfusion and T2*-perfusion MRI. *PloS One* 2019;**14**(4):e0215400. https://doi.org/10.1371/journal.pone.0215400.
8. Zhou J, Heo HY, Knutsson L, van Zijl PCM, Jiang S. APT-weighted MRI: techniques, current neuro applications, and challenging issues. *J Magn Reson Imag* 2019;**50**(2):347–64. https://doi.org/10.1002/jmri.26645.
9. van Zijl PCM, Lam WW, Xu J, Knutsson L, Stanisz GJ. Magnetization transfer contrast and chemical exchange saturation transfer MRI. Features and analysis of the field-dependent saturation spectrum. *Neuroimage* 2018;**168**:222–41. https://doi.org/10.1016/j.neuroimage.2017.04.045.
10. Jiang S, Eberhart CG, Zhang Y, Heo HY, Wen Z, Blair L, et al. Amide proton transfer-weighted magnetic resonance image-guided stereotactic biopsy in patients with newly diagnosed gliomas. *Eur J Canc* 2017;**83**:9–18. https://doi.org/10.1016/j.ejca.2017.06.009.
11. Yu H, Wen X, Wu P, Chen Y, Zou T, Wang X, et al. Can amide proton transfer-weighted imaging differentiate tumor grade and predict Ki-67 proliferation status of meningioma? *Eur Radiol* 2019;**29**(10):5298–306. https://doi.org/10.1007/s00330-019-06115-w.
12. Zou T, Yu H, Jiang C, Wang X, Jiang S, Rui Q, et al. Differentiating the histologic grades of gliomas preoperatively using amide proton transfer-weighted (APTW) and intravoxel incoherent motion MRI. *NMR Biomed* 2018;**31**(1):10. https://doi.org/10.1002/nbm.3850.
13. Jiang S, Eberhart CG, Lim M, Heo HY, Zhang Y, Blair L, et al. Identifying recurrent malignant glioma after treatment using amide proton transfer-weighted MR imaging: a validation study with image-guided stereotactic biopsy. *Clin Canc Res* 2019;**25**(2):552–61. https://doi.org/10.1158/1078-0432.Ccr-18-1233.
14. He YL, Li Y, Lin CY, Qi YF, Wang X, Zhou HL, et al. Three-dimensional turbo-spin-echo amide proton transfer-weighted mri for cervical cancer: a preliminary study. *J Magn Reson Imag* 2019;**50**(4):1318–25. https://doi.org/10.1002/jmri.26710.
15. Dula AN, Arlinghaus LR, Dortch RD, Dewey BE, Whisenant JG, Ayers GD, et al. Amide proton transfer imaging of the breast at 3 T: establishing reproducibility and possible feasibility assessing chemotherapy response. *Magn Reson Med* 2013;**70**(1):216–24. https://doi.org/10.1002/mrm.24450.
16. Jia G, Abaza R, Williams JD, Zynger DL, Zhou J, Shah ZK, et al. Amide proton transfer MR imaging of prostate cancer: a preliminary study. *J Magn Reson Imag* 2011;**33**(3):647–54. https://doi.org/10.1002/jmri.22480.
17. Togao O, Hiwatashi A, Yamashita K, Kikuchi K, Keupp J, Yoshimoto K, et al. Grading diffuse gliomas without intense contrast enhancement by amide proton transfer MR imaging: comparisons with diffusion- and perfusion-weighted imaging. *Eur Radiol* 2017;**27**(2):578–88. https://doi.org/10.1007/s00330-016-4328-0.
18. Park JE, Kim HS, Park KJ, Kim SJ, Kim JH, Smith SA. Pre- and posttreatment glioma: comparison of amide proton transfer imaging with MR spectroscopy for biomarkers of tumor proliferation. *Radiology* 2016;**278**(2):514–23. https://doi.org/10.1148/radiol.2015142979.
19. Lee JB, Park JE, Jung SC, Jo Y, Kim D, Kim HS, et al. Repeatability of amide proton transfer-weighted signals in the brain according to clinical condition and anatomical location. *Eur Radiol* 2020;**30**(1):346–56. https://doi.org/10.1007/s00330-019-06285-7.
20. van de Ven K, Keupp J. Amide Proton Transfer weighted imaging: Advancement in molecular tumor diagnosis (White paper).Philips; http://images.philips.com/is/content/PhilipsConsumer/Campaigns/HC20140401_DG/HC-Master-White_paper_3D_APT_14062018.PDF?_ga=2.90840083.821747877.1599558254-1462602917.1599558254.
21. Jahng GH, Li KL, Ostergaard L, Calamante F. Perfusion magnetic resonance imaging: a comprehensive update on principles and techniques. *Korean J Radiol* 2014;**15**(5):554–77. https://doi.org/10.3348/kjr.2014.15.5.554.
22. Scheidegger R, Wong ET, Alsop DC. Contributors to contrast between glioma and brain tissue in chemical exchange saturation transfer sensitive imaging at 3 Tesla. *Neuroimage* 2014;**99**:256–68. https://doi.org/10.1016/j.neuroimage.2014.05.036.

23. Chan YH. Biostatistics 104: correlational analysis. *Singap Med J* 2003;**44**(12):614–9.
24. de Vet HC, Terwee CB, Knol DL, Bouter LM. When to use agreement versus reliability measures. *J Clin Epidemiol* 2006;**59**(10):1033–9. https://doi.org/10.1016/j.jclinepi.2005.10.015.
25. Koo TK, Li MY. A guideline of selecting and reporting intraclass correlation coefficients for reliability research. *J Chiropr Med* 2016;**15**(2):155–63. https://doi.org/10.1016/j.jcm.2016.02.012.
26. Gerke O. *Reporting standards for a bland-altman agreement analysis: a review of methodological reviews***10**; 2020. p. 334. https://doi.org/10.3390/diagnostics10050334. 2075-4418 (Print).
27. Abu-Arafeh A, Jordan H, Drummond G. Reporting of method comparison studies: a review of advice, an assessment of current practice, and specific suggestions for future reports. *Br J Anaesth* 2016;**117**(5):569–75. https://doi.org/10.1093/bja/aew320.
28. Park YW, Ahn SS, Kim EH, Kang SG, Chang JH, Kim SH, et al. Differentiation of recurrent diffuse glioma from treatment-induced change using amide proton transfer imaging: incremental value to diffusion and perfusion parameters. *Neuroradiology* 2020. https://doi.org/10.1007/s00234-020-02542-5. 10.1007/s00234-020-02542-5.
29. Zhou J, Tryggestad E, Wen Z, Lal B, Zhou T, Grossman R, et al. Differentiation between glioma and radiation necrosis using molecular magnetic resonance imaging of endogenous proteins and peptides. *Nat Med* 2011;**17**(1):130–4. https://doi.org/10.1038/nm.2268.
30. Park KJ, Kim HS, Park JE, Shim WH, Kim SJ, Smith SA. Added value of amide proton transfer imaging to conventional and perfusion MR imaging for evaluating the treatment response of newly diagnosed glioblastoma. *Eur Radiol* 2016;**26**(12):4390–403. https://doi.org/10.1007/s00330-016-4261-2.
31. Law M, Young R, Babb J, Pollack E, Johnson G. Histogram analysis versus region of interest analysis of dynamic susceptibility contrast perfusion MR imaging data in the grading of cerebral gliomas. *AJNR Am J Neuroradiol* 2007;**28**(4):761–6.
32. Oei MTH, Meijer FJA, Mordang JJ, Smit EJ, Idema AJS, Goraj BM, et al. Observer variability of reference tissue selection for relativecerebral blood volume measurements in glioma patients. *Eur Radiol* 2018;**28**(9):3902–11. https://doi.org/10.1007/s00330-018-5353-y.
33. Smits M, Bendszus M, Collette S, Postma LA, Dhermain F, Hagenbeek RE, et al. Repeatability and reproducibility of relative cerebral blood volume measurement of recurrent glioma in a multicentre trial setting. *Eur J Canc* 2019;**114**:89–96. https://doi.org/10.1016/j.ejca.2019.03.007.
34. Togao O, Yoshiura T, Keupp J, Hiwatashi A, Yamashita K, Kikuchi K, et al. Amide proton transfer imaging of adult diffuse gliomas: correlation with histopathological grades. *Neuro Oncol* 2014;**16**(3):441–8. https://doi.org/10.1093/neuonc/not158.
35. Wen Z, Hu S, Huang F, Wang X, Guo L, Quan X, et al. MR imaging of high-grade brain tumors using endogenous protein and peptide-based contrast. *Neuroimage* 2010;**51**(2):616–22. https://doi.org/10.1016/j.neuroimage.2010.02.050.
36. Leao DJ, Craig PG, Godoy LF, Leite CC, Policeni B. Response assessment in neurooncology criteria for gliomas: practical approach using conventional and advanced techniques. *AJNR Am J Neuroradiol* 2020;**41**(1):10–20. https://doi.org/10.3174/ajnr.A6358.
37. Schön S, Cabello J, Liesche-Starnecker F, Molina-Romero M, Eichinger P, Metz M, et al. Imaging glioma biology: spatial comparison of amino acid PET, amide proton transfer, and perfusion-weighted MRI in newly diagnosed gliomas. *Eur J Nucl Med Mol Imag* 2020;**47**(6):1468–75. https://doi.org/10.1007/s00259-019-04677-x.